Available online at www.sciencedirect.com

SciVerse ScienceDirect

Physics Procedia 37 (2012) 205 – 212

Physics Procedia

TIPP 2011 - Technology and Instrumentation in Particle Physics 2011

Calibration of the ATLAS hadronic barrel calorimeter TileCal using 2008, 2009 and 2010 cosmic-ray muon data

Zhili Weng[a,b] [1] on behalf of the ATLAS Tile Calorimeter group

[a] *Institute of Physics, Academia Sinica, TW - Taipei 11529, Taiwan.*
[b] *School of Physics and Engineering, Sun Yat-sen University, Guangzhou, PR China.*

Abstract

The ATLAS iron-scintillator hadronic calorimeter (TileCal) provides precision measurements of jets and missing transverse energy produced in the LHC proton-proton collisions. Results assessing the calorimeter calibration obtained using cosmic ray muons collected in 2008, 2009 and 2010 are presented. The analysis was based on the comparison between experimental and simulated data, and addresses three issues. First the average non-uniformity of the response of the cells within a layer was estimated to be about ±2%. Second, the average response of different layers was found to be not inter-calibrated, considering the sources of error. The largest difference between the responses of two layers was 4%. Finally, the differences between the energy scales of each layer obtained in this analysis and the value set at test beams using electrons was found to range between -3% and +1%. The sources of uncertainties in the response measurements were strongly correlated, including the uncertainty in the simulation. The total error of each layer determinations was 2%. Stable response values were obtained for the three data-taking periods. The uncertainties on the comparisons were less than ±1% for the Long Barrel layers and less than ±3% for the Extended Barrel ones.

Keywords: ATLAS, Calorimeter, TileCal, Cosmic Rays, Calibration

1. Introduction

Cosmic-ray muon events were collected by the ATLAS experiment [1] in 2008, 2009 and 2010. The data have been used to validate the calibration of the hadronic calorimeter TileCal [2]. The studies of cosmic-ray muons provide an independent and direct method to cross-check the calibration done by different procedure and quantify possible residual systematics in a very clean environment. The interaction of muons with matter is well understood. The energy of the muons have been selected so that the dominant energy loss process is ionization [3] and the energy loss is essentially proportional to the muon track path length. The response of the detector has been studied determining the ratio between the energy deposited in a calorimeter cell (dE) and the track path-length in the cell (dl).

[1] Email: zhili.weng@cern.ch

1875-3892 © 2012 Published by Elsevier B.V. Selection and/or peer review under responsibility of the organizing committee for TIPP 11. Open access under CC BY-NC-ND license. doi:10.1016/j.phpro.2012.03.709

2. The Tile Calorimeter

The ATLAS detector at the Large Hadron Collider (LHC) covers almost the whole solid angle around the collision point with tracking detectors, calorimeters and muon chambers. It was designed to study a wide range of physics topics at LHC energies.

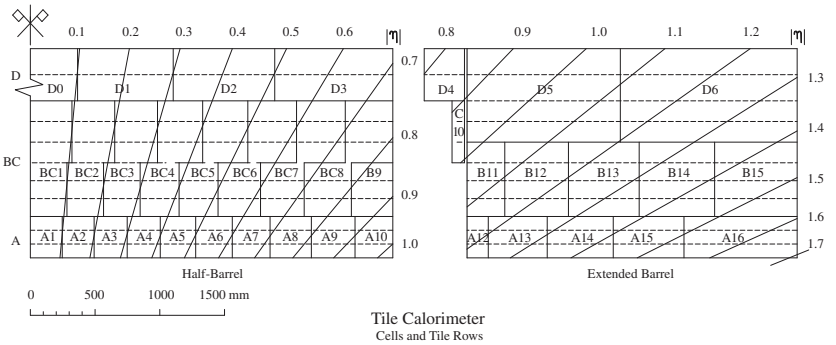

Fig. 1. Long Barrel (LB) (left) and Extended Barrel (EB) sections of the calorimeter. Horizontal dashed lines delineate the 11 rows of scintillating tiles. Full horizontal lines define the three radial layers. Full vertical lines show the cell boundaries. Also shown are lines of fixed pseudorapidity.

The ATLAS hadronic barrel calorimeter TileCal [2] is a sampling plastic-scintillator/steel calorimeter. It is divided into three cylindrical sections, referred to as the Long Barrel (LB) and Extended Barrels (EB), altogether covering the region $|\eta| < 1.6$. Each of the three sections is composed of 64 azimuthal segments, referred to as modules, subtending $\Delta\phi = 2\pi/64 \approx 0.0982$. The TileCal plates, made of iron and plastic-scintillators, are placed perpendicular to the proton beam axis (z direction) and are radially staggered in depth. The scintillating tiles are 3 mm thick and the total thickness of the iron plates in one 18 mm period is 14 mm. The modules are segmented in z and in radial depth. This segmentation defines a quasi-projective tower structure, in which the deviations from perfect projectivity are small compared to the typical angular size of hadronic jets. In total, TileCal comprises 5182 readout cells. The layout of the cells is shown in Fig. 1. The 6 radial layers will be referred to in the following anlysis as: LB-A, LB-BC, LB-D for the Long Barrel, and EB-A, EB-B, EB-D for the Extended Barrels.

3. The analysis of the data

About one million events were analyzed in each data period. The muon tracks reconstructed using the inner tracking detector [4] (Pixel and SCT) were extrapolated through the volume of the calorimeter using the method described in Ref. [5]. The extrapolation was performed following both directions, downstream and upstream of the reconstructed muon track. Additional linear interpolation, using the detailed cell geometry model, was used to determine the entry and exit points of the muon in every crossed cell. The track path length dl was then evaluated as the distance between these points for every cell.

The deposited energy dE in a single cell was determined using the Optimal Filtering Coefficients Method [6]. The electro-magnetic (EM) scale factor (1.050 pC/GeV), which converts the measured signal to the deposited energy, was determined at test beams using electron beams directed on the center of each cell with an angle of 20°. The estimated error on this factor is 0.5% [7]. It was transferred to ATLAS by means of the ^{137}Cs source calibration procedure. Corrections due to the magnetic field effect and to the increase or "up-drift" of the PMTs response to a radioactive ^{137}Cs source, up to about 1% in average in one year, were applied [6].

3.1. Selection criteria

The selection criteria applied to both Data and Monte Carlo simulation (MC) for this analysis require: clean event with good quality tracks; muon momentum range $10 < p < 30$ GeV, to stay out of multiple

scattering and radiative energy losses; geometrical cut to ensure the muon track was well contained inside the analysing cells and crossing several iron plates and scintilators; minimum dE cut at 2σ of the cell noise (60 MeV). Unless explicitly stated otherwise, only cells downstream in the lower part of the calorimeter were used to quote the result, in order to have a better path reconstruction.

3.2. The Monte Carlo simulation

A Monte Carlo simulation study of the cosmic-ray muon events was performed. The MC uses the Geant4 toolkit [8] [9], which provides the physics model(s) of particle interactions with material, the ATLAS geometry description [2] and the tracking tools. The MC uses the cosmic-ray muon spectrum as measured at sea level [10]. The behavior of the front-end electronics (pulse shaping, electronic noise and digitization) is emulated allowing the energy reconstruction procedure to be applied to the simulated events as well. Two million MC cosmic-ray muon events were produced, about twice the event statistics in each data period. On average, the simulated and experimental spectra (momentum, angular) are consistent within a few percent.

3.3. The Calorimeter response

The response of the cells in the LB-BC layer is shown in Fig. 2a) as a function of the track path length dl. A fit to the corresponding profile histogram shows that the muon response scales linearly with the path length to a good approximation. This result suggests that the ratio dE/dl is a suitable quantity to study the calorimeter inter-calibration.

The experimental and the simulated distributions of this quantity for cells LB-D2 (see Fig. 1) are shown in Fig. 2b) as an example. The curve shown in the figure is fit of Landau functions, convoluted with Gaussians, to the data. It is found that the fitted function does not describe the distributions over the whole range and thus may yield biases in evaluating parameters such as the peak value. For this reason a truncated mean, $\langle dE/dl\rangle_t$, was used to define the muon response. For each TileCal cell it was computed by truncating a fraction (F =1%) of entries in the upper side of the dE/dl distributions. The truncated mean was preferred to the full one because it is less affected by rare energy-loss processes such as energetic δ-rays, which can cause large fluctuations on the mean. It is noteworthy that the truncated mean exhibits a slight non-linear scaling with the path length dl. This non-linearity and other residual non-uniformities such as differences in momentum and incident angle spectra are, to a large extent, reproduced by the MC. To compensate for these effects the ratio between the experimental and simulated truncated means

$$R = \frac{\langle dE/dl\rangle_t}{\langle dE/dl\rangle_t^{MC}} \tag{1}$$

was defined for each calorimeter cell. In the following sections the calorimeter response equalization and the EM scale setting are always investigated using this quantity.

4. Results

The experimental results: a) uniformity of the response of the cells of a layer, b) layer inter-calibration, c) stability of the response in three data periods and d) EM scale measurement, are discussed in this section.

4.1. Uniformity of the calorimeter cell response

The cosmic-ray muons probe the cells uniformly over the entire volume and can give a response representative of the average cell light yield. The inter-calibration of the cells in each layer was tested by comparing the corresponding experimental and simulated dE/dl distributions. The ratios of the truncated means, $R_c^l = (\langle dE/dl\rangle_t/\langle dE/dl\rangle_t^{MC})_c^l$, were computed for a large number of cells c. The upper region of the detector was included. The index l runs over the three layers of the barrel, LB-A (l = 1) (see Figure 3), LB-BC (l = 2), LB-D (l = 3), and the extended barrel EB-A (l = 4), EB-B (l = 5) and EB-D (l = 6). Cells crossed by more than 100 cosmic-ray muon tracks were used. For each data set period only the layers with a total number of cells that satisfy these conditions, N_c^l, larger than 20 were retained. The N_c^l values range between $\approx$ 30 (5% of the layer cells) for EB-B and $\approx$ 550 (45% of the layer cells) for LB-BC.

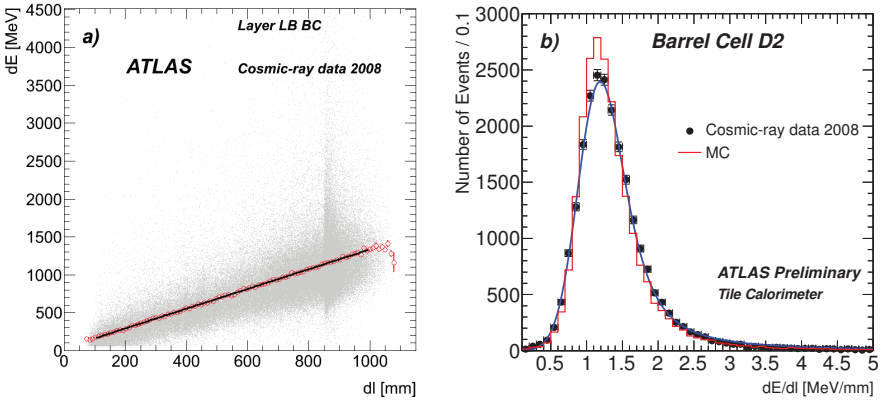

Fig. 2. a) Response of the barrel module LB-BC cells as a function of track path length obtained using 2008 data. The solid line corresponds to a linear fit to the averaged response in each path length bin showen in red circle. b) Example distribution of the quantity dE/dl for the cells LB-D2 obtained using 2008 data (full points) and simulated data (solid lines).

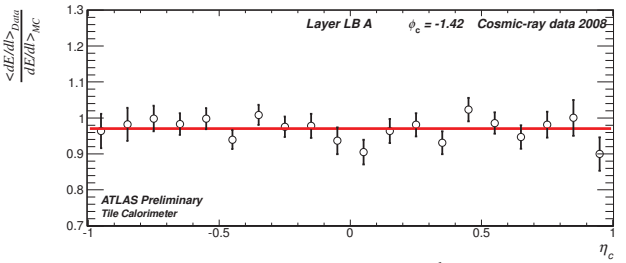

Fig. 3. Data/MC Ratio of the truncated means of dE/dl by cosmic-ray muons, R_c^l, obtained using 2008 experimental and simulated data as a function of the pseudorapidity η_c. Only cells LB-A of the module with azimuth angle ϕ_c = -1.42 are shown.

The dispersion of the cells around the average is a measure of a possible non-uniformity of the cell response not described in the MC. The hypothesis H_0, that the cells of each layer l are inter-calibrated was statistically tested using the minimum of the χ^2 function [3]:

$$\chi^2 = \sum^{N_c^l} \frac{(R_c^l - \mu^l)^2}{(\sigma_c^l)^2}. \tag{2}$$

The parameters μ^l were determined in the minimization, and σ_c^{l2} denote the relevant statistical errors. For each layer, a p-value is obtained by minimizing Eq.(2) which represents the probabilities of observing competible or larger cell fluctuation from hypothesis H_0. Apart from the layer EB-B, the p-values were very small ($< 10^{-5}$) indicating that the cells fluctuate more than expected by statistical uncertainties.

This additional non-uniformity of the cells in a layer, s^l, was determined by the Maximum Likelihood method. Assuming that the quantities R_c^l follow a Gaussian distribution, the Likelihood function

$$L = \prod_{c=1}^{N_c^l} \frac{1}{\sqrt{(\sigma_c^{l2} + s^{l2})2\pi}} e^{-\frac{1}{2}\left(\frac{R_c^l - \mu^l}{\sqrt{\sigma_c^{l2} + s^{l2}}}\right)^2} \tag{3}$$

was maximized. The horizontal line shown in Figs. 3 corresponds to the resulting $\hat{R}_c^l$ values.

As a result, the additional term s^l was compatible with 0 for EB-B, which was consistent with the χ^2 test results. For the other layers, this factor was estimated to be about 0.02.

This additional term is a combined effect of various factors, such as systematic errors due to limitations of the simulation and spreads in cell inter-calibration. In particular the MC simulation has no variations in the quality of the optical components of the calorimeter or in the channel signal shape. The resulting values of s^l were then interpreted as upper limits on the average non-uniformity of the cells of a layer. It

is worthwhile to recall that a similar degree of non-uniformity was obtained by studying the calorimeter response to electron test beams [7].

4.2. Inter-calibration of the radial layers

In order to have a more reliable determination, the dE/dl distributions were determined using all the cells of a layer. For each period, the number of tracks per layer measured in each layer range from 7k (EB) to 100k (LB). The largest difference between the response of two layers was 4%. The LB measurements were in agreement with the ones obtained at the test beams using projective muons [6].

Layer	R^l 2008 data	R^l 2009 data	R^l 2010 data
LB-A	0.966 ± 0.012	0.972 ± 0.015	0.971 ± 0.011
LB-BC	0.976 ± 0.015	0.981 ± 0.019	0.981 ± 0.015
LB-D	1.005 ± 0.014	1.013 ± 0.014	1.010 ± 0.013
EB-A	0.964 ± 0.043	0.965 ± 0.032	0.996 ± 0.037
EB-B	0.977 ± 0.018	0.966 ± 0.016	0.988 ± 0.014
EB-D	0.986 ± 0.012	0.975 ± 0.012	0.982 ± 0.014

Table 1. Values of the ratios of the truncated means R^l obtained for the different layers analyzing the three data sets periods. The uncertainty corresponds to the square root of the diagonal elements of the error matrices (see text).

Systematic effects have been investigated to establish the significance of the observed differences in response. Correlation of the errors have been taken into account. Ten sources of systematic uncertainties were considered, 6 of which are related to the event selection criteria. This type of systematic effect was studied by varying the dominant parameters in a wide range of kinematical and geometrical selection regions.

In addition, the uncertainties of the method applied to determine the detector response to cosmic-ray muons were considered by changing the truncation or the shape(width) of the distribution. The effect of the different spread of the experimental and simulated dE/dl distributions on the determination of the truncated means was estimated to be equal to 0.3% using a toy MC.

The third class of uncertainties, concerns the signal calibration procedures performed at the test beam and in-situ at ATLAS. 1) The uncertainty on the calibration radial correction measured in test beams using 90° muons [7] was estimated to be 0.3%. 2) The cell read-out up-drift and magnetic field effect determinations were assigned a systematic correlated uncertainty equal to 1% and 0.6% in the LB and EB cells, respectively.

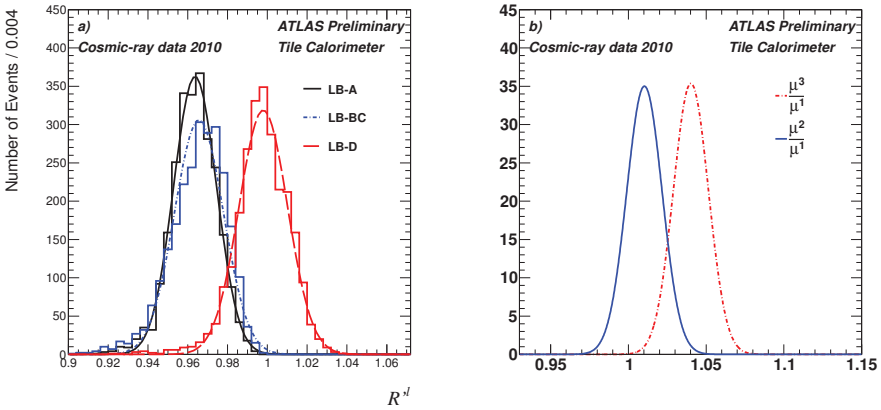

Fig. 4. a) Distributions of the pseudo-measurement ratios of the truncated means of dE/dl. The 2010 results of the Barrel layers LB-A, LB-BC and LB-D are shown. The curves correspond to Gaussian functions fit to the data.b) Posterior PDF of the model parameters ratios μ^2/μ^1 (solid curve) and μ^3/μ^1 (dot-dashed curve) obtained using 2010 data (see text).

After identifying the source of the errors, systematic parameters, S_m, were considered as random variables [11] and their values were selected according to the predefined distributions. In the case of the uncorrelated errors different value of S_m was used for each layer. Each combination of the parameters was used to generate a pseudo-measurement R'^l ($l = 1, ..., 6$). The distributions obtained using 2010 data for the layers LB-A, LB-BC and LB-D are reported in Fig. 4a). The curves correspond to Gaussian functions fit. The error matrix V was determined using the equation

$$V^{l,l'} = \frac{\sum_{i=1}^{N}(R'^l - \hat{R'^l})(R'^{l'} - \hat{R'^{l'}})}{N}, \tag{4}$$

where N, equal to 2500, is the number of pseudo-measurements and $\hat{R'^l}$ the averages of the distributions. Similar results were found for the three years data sets. The measurement uncertainties in Table 1 correspond to the square root of the diagonal error matrix elements. The absolute values of the corresponding correlation matrix elements can be as high as 100%, indicating large correlations between the effects of a given cut in different layers.

A model with six parameters, μ^l (l=1, ..., 6), which denotes the true response for each layer, was considered. According to the Bayes theorem the parameter values can be inferred from the R^l measurements reported in Table 1 using the equation

$$f(\mu^1, ..., \mu^6 \mid R^1, ..., R^6) = \frac{f(R^1, ..., R^6 \mid \mu^1, ..., \mu^6) f_0(\mu^1, ..., \mu^6)}{\int f(R^1, ..., R^6 \mid \mu^1, ..., \mu^6) f_0(\mu^1, ..., \mu^6) d\mu^1 .... d\mu^6} \tag{5}$$

where the probability function (PDF) of the measurements, for given values of μ^1, ..., μ^6, $f(R^1, ..., R^6 \mid \mu^1, ..., \mu^6)$, is equal to the likelihood function $\mathcal{L}(\mu^1, ..., \mu^6; R^1, ..., R^6)$. Due to a "vague" prior knowledge of the parameters, a flat prior probabilities $f_0(\mu^1, ..., \mu^6)$ [11] were used. Since the R^l distributions are near Gaussian (see Fig. 4b)), the six layer measurements, $R^1, ..., R^6$ were assumed to be representative of a six-dimension Gaussian function:

$$f(\mu^1, ..., \mu^6 \mid R^1, ..., R^6) = K\mathcal{L}(\mu^1, ..., \mu^6; R^1, ..., R^6) = K' e^{[-\frac{1}{2}(\vec{R}-\vec{F})^T V^{-1}(\vec{R}-\vec{F})]} \tag{6}$$

where K and K' are normalization factors, $\vec{R} = (R^1, ..., R^6)$ and $\vec{F} = (\mu^1, ..., \mu^6)$ are column vectors. The superscript T denotes a row vector. The quantity V^{-1} was the inverse of the error matrix (see Eq. 4).

For each pair of layers, l and l', the posterior PDF $f(\mu^l, \mu^{l'} \mid R^1, ..., R^6)$ was computed integrating numerically Eq. (6) over the other layer parameters. As shown in Fig. 4, the PDF of the 2010 data ratios $\mu^l/\mu^{l'}$ are well described by Gaussian functions. The mean values and the RMS of the distributions were calculated. All the results were compatible with unity, except the ratios μ^3/μ^1 and μ^3/μ^2 that differ from unity of about 4 and 3 standard deviations respectively. Similar results were obtained analyzing 2008 and 2009 data. One can conclude that it is unlikely that the layer LB-D is equalized to the layers LB-A and LB-BC. On the basis of this analysis the layers LB-A, LB-BC, EB-A, EB-B and EB-D were inter-calibrated. The stability of the results was checked using different distributions of the systematic parameters S_m.

4.3. Stability of the layer response

The TileCal response could evolve with time due to: a) PMT response drift, b) aging effects of the scintillator and WLS fibres and c) damage effects due to radiation or mechanical changes in the coupling of the optical components. As already mentioned, a decrease of the response of the detector of about 1% per year was monitored using the laser and ^{137}Cs systems. The cosmic-ray muon data allowed for the validation of the adjustments performed in the period 2008-2010.

The results discussed in Sections 4.1 and 4.2 show that the TileCal response was quite stable over the three years studied. The method described in Section 4.2 was used to quantify the stability of the layer response, R^l, as a function of time. For each layer l the measurements R^l_y obtained in the three years y=2008, y=2009, and y=2010 were compared. The posterior distribution used was

$$f(\mu^l_{2008}, \mu^l_{2009}, \mu^l_{2010} \mid R^l_{2008}, R^l_{2009}, R^l_{2010}) = Ke^{[-\frac{1}{2}(\vec{P}-\vec{G})^T W^{-1}(\vec{P}-\vec{G})]} \tag{7}$$

where K is a normalization factor and $\vec{P} = (R^l_{2008}, R^l_{2009}, R^l_{2010})$. The quantity $\vec{G} = (\mu^l_{2008}, \mu^l_{2009}, \mu^l_{2010})$ is the vector of the model parameters corresponding to the components of the mean value of a three dimensional Gaussian function. The error matrix W describes the uncertainties and the correlations of the measurements performed in the different years. This was obtained by analyzing the effect of the selection criteria as described in Section 4.2. All of the determinations $\mu^l_y/\mu^l_{y'}$ were consistent with 1.00 and the maximum deviation was at 2 sigma level. The uncertainties of the LB comparisons were close to the PMT's average up-drift measured with ^{137}Cs in one year (see Section 3). One can conclude that within the present uncertainties, the response of the calorimeter to cosmic-ray muons was stable over the three years studied.

4.4. The Electromagnetic energy scale test

The energy scale of TileCal was determined using beams of electrons at test beams and transported to ATLAS using measurements performed with a ^{137}Cs source. The scale was defined in an analogous way in the MC simulation. The response of electrons was simulated in a setup similar to the test beam one and the incident particle energy was used to define the MC conversion factor. The ratio between the data and the simulated response to muons, Eq. (1), is expected to be equal to 1 and any deviation is attributed to a difference between the current scale in ATLAS, EM_{ATLAS}, and the one set at test beams, EM

$$R^l = R^l_{EM} = \frac{EM^l_{ATLAS}}{EM}. \tag{8}$$

To identify the possible sources of systematic errors, the R^l ratios can be expressed by making more explicit all the factors which affect the scale setting:

$$R^l_{EM} = \left(\frac{\langle dE/dl\rangle_t}{\langle dE/dl\rangle^{MC}_t}\right)^l = \left(\frac{\langle dE_{pC}/dl\rangle_t}{\langle dE_{dep}/dl\rangle^{MC}_t}\right)^l \times \frac{E^{eMC}_{dep}}{E^{eMC}} \times \frac{f_{instr}}{f^e_{instr}} \times \frac{E^{eTB}}{E^{eTB}_{pC}} \tag{9}$$

where dE_{pC} is the signal in pC produced in a cell by cosmic-ray muons, E^{eTB}_{pC} is the signal measured in pC produced by electrons with energy E^{eTB} in the range 20 to 180 GeV impinging on the cells at 20°, dE_{dep} is the simulated energy deposited in the active material of a cell by cosmic-ray muons, E^{eMC}_{dep} is the simulated energy deposited by electrons with energy E^{eMC} in the range 20 to 180 GeV impinging on the cells at 20° and $EM = E^{eTB}_{pC}/E^{eTB}$. For the signals measured in pC, the inter-calibration of the electronics read-out is already taken into account by the Charge Injection System (CIS) [6] and the inter-calibration of the cell light yield and PMT gain equalization are addressed with the ^{137}Cs source. The ratio R_{instr}=f_{instr}/f^e_{instr} describes the differences of the response of the detector to cosmic-ray muons and calibration electrons.

The systematic uncertainties needed to be considered are: 1) The uncertaintiy (Δ_{cosm}) on the cosmic-ray muons analysis; 2) The uncertainty (Δ_{cal}) on the determination of the EM scale at the TBs and its transportation to ATLAS; 3) The uncertainty (Δ_{MC}) on the simulation of the muon and electron calorimeter response. The errors Δ_{cal} and Δ_{MC} affect all the determinations of R^l in a correlated way and hence were not considered in the inter-calibration studies.

The uncertainty Δ_{cal}, reported in Table 2, was obtained by combining in quadrature the uncertainties on: The EM scale (0.5%) [7]; The propagation of the calibration of the ^{137}Cs readout gain from the test beam to ATLAS (0.2%) [6]; The propagation of the calibration of the digital readout by CIS 0.1% [6].

The simulation of the muons was based on the Geant4 QGSP_BERT physics list. The systematic errors associated to specific transportation code can be determined using special simulations of muons and electrons in which different parameters or models are used. The two most important sources of systematic uncertainty in the simulation are: the use of tracking cuts on the low energy secondaries and the choise of multiple-scattering model used in the simulation. These two systematic effect on the R_{dep} ratio was estimated to be ±1.2%. In addition, the effects of the gamma-nuclear and lepto-nuclear interactions have been considered, and found to be about ±0.4%.

The instrumental effects f_{instr} (f^e_{instr}) considered in the case of muons (electrons) in Eq. (9) are: Systematic error from saturation effects described by the Birks law [12], the PMT photo-statistics effect and the light attenuation in the fibres.

The uncertainties have been combined in quadrature to obtain the error Δ_{MC} reported in Table 2.

Layer	$R^l_{EM} = EM^l_{ATLAS}/EM$	Δ_{cosm}	Δ_{cal}	Δ_{MC}	Δ_{Tot}
LB-A	0.971	± 0.011	±0.005	±0.013	±0.018
LB-BC	0.981	± 0.015	±0.005	±0.013	±0.020
LB-D	1.010	± 0.013	±0.005	±0.013	±0.019
EB-A	0.996	± 0.037	±0.005	±0.013	±0.040
EB-B	0.988	± 0.014	±0.005	±0.013	±0.020
EB-D	0.982	± 0.014	±0.005	±0.013	±0.020

Table 2. Ratio R^l_{EM} between the actual value of the energy scale from this analysis and the value obtained at test beams using elecron range between -3% and +1%. The uncertainty in the third column is the square root of the diagonal elements of the error matrix (see Eq. (4)). The total error obtained by combining in quadrature the three effects is reported in the last column. Only Result for 2010 is shown, similar results were obtained using 2008 and 2009 data.

5. Summary and conclusions

Cosmic-ray muon events collected in 2008, 2009 and 2010 have been used in the ATLAS experiment to test the calibration of the hadronic barrel calorimeter TileCal. The analysis was based on the comparison between experimental and simulated data.

Upper limits on the average non-uniformity of the response of the cells in a layer were estimated to be ±2%. In the study of the layer inter-calibration the systematic error due to the cosmic-ray muon measurements and to the TileCal calibration procedure were considered. A maximal deviation of 4% was observed. A Bayesian statistical method showed that the layer LB-D response differs from that of LB-A and LB-BC by about 4 and 3 standard deviations, respectively. The responses of all the other layer pairs were consistent.

The differences between the values of the layer energy scale obtained in this analysis and the one set at test beams using electrons ranged between -3% and +1%. The sources of uncertainty in the response measurements were strongly correlated, and include the uncertainty in the simulation of the muon response. The total error of each layer determination represented by the value of the diagonal elements of the error matrix was at the order of 2%.

Stable results were obtained for the three periods. They show that the ^{137}Cs system was able to follow the variations of the PMTs gain and to compensate for the drift of the response at a level better than 1% and 3% in the LB and EB respectively.

6. Acknowledgment

I would like to thank the Technology and Instrumentation in Particle Physics 2011 organizers and the Tile Calorimeter Speakers Committee for giving me the chance to present this study on behalf of the ATLAS Tile Calorimeter group in the coference. I would also like to thank Claudio Santoni for his help in preparing this proceeding.

References

[1] ATLAS Collaboration, The ATLAS Experiment at the CERN Large Hadron Collider, JINST 3 (2008) S08003.
[2] ATLAS Collaboration, Tile Calorimeter Technical Design Report, CERN, Geneva, Switzerland, CERN/LHCC 96-42.
[3] C. Amsle *et al.*, Physics Letters B 667 1 (2008).
[4] ATLAS Collaboration, Inner detector Technical Design Report, CERN, Geneva, Switzerland, Volume I CERN/LHCC 97-16, Volume II CERN/LHCC 97-17.
[5] E. Lund *et al.*, Track parameter Propagation through the Application of a new adaptive Runge-Kutta-Nystrom Method in the ATLAS experiment, ATLAS Note ATL-SOFT-PUB-2009-001 (2009).
[6] The ATLAS Collaboration, Readiness of the ATLAS Tile Calorimeter for LHC collisions, Eur. Phys. J. C 70 1193-1236 (2010)
[7] P. Adragna *et al.*, Nucl. Instr. and Meth. A 606 (2009) 362-394.
[8] S. Agostinelli *et al.*, Methods in Physics Research A 506 (2003) 250-303.
[9] J. Allison *et al.*, IEE Transactions on Nuclear Science 53 No. 1 (2006) 270-278.
[10] A. Dar, Phys. Rev. Lett. 51 (1983) 227-230.
[11] G. D'Agostini, Bayesian Reasoning in High-Energy Physiscs: Principles and Applications, CERN 99-03 (1999).
[12] J.B. Birks, The theory and practice of scintillation counting, Oxford, Pergamon Press, 1964.
[13] E. Starchenko *et al.*, Nucl. Instr. and Meth. A 494 (2002) 281-284.